Dispersion relation of coupled-resonator acoustic waveguides formed by defect cavities in a phononic crystal

2013 J. Phys. D: Appl. Phys. 46 475301

(http://iopscience.iop.org/0022-3727/46/47/475301)

IOP PUBLISHING JOURNAL OF PHYSICS D: APPLIED PHYSICS

J. Phys. D: Appl. Phys. **46** (2013) 475301 (7pp) doi:10.1088/0022-3727/46/47/475301

Dispersion relation of coupled-resonator acoustic waveguides formed by defect cavities in a phononic crystal

Jose Maria Escalante[1], **Alejandro Martínez**[1] **and Vincent Laude**[2]

[1] Nanophotonics Technology Center, Universitat Politècnica de Valencia, Valencia 46022, Spain
[2] Institut FEMTO-ST, Université de Franche-Comté and CNRS, Besançon, France

E-mail: jmescala@ntc.upv.es

Received 28 June 2013, in final form 6 September 2013
Published 31 October 2013
Online at stacks.iop.org/JPhysD/46/475301

Abstract

We investigate the dispersion of phononic crystal waveguides formed by evanescent coupling of a chain of defect cavities and supporting slow-wave propagation. These coupled-resonator acoustic waveguides (CRAWs) are analogous to the coupled-resonator optical waveguides formed in photonic crystals. CRAW dispersion can be controlled by increasing the distance between cavities, with the result of decreasing their coupling, and hence flattening the dispersion relation. Based on the tight-binding model, the dispersion relation is found in the form of a Fourier series expansion with explicitly given coefficients. This model is tested against the exact dispersion relation of a two-dimensional solid–solid phononic crystal of tungsten inclusions in a silicon matrix and only partial agreement is found. An alternative model of a linear chain of coupled resonators, resting only on the hypotheses of linearity and periodicity, is then proposed. While the Fourier coefficients in this model are *a priori* unspecified, they can be fitted against the exact dispersion relation, resulting in an excellent agreement with only a few terms in the Fourier series expansion. The Fourier coefficients are shown to be a direct measure of the coupling of neighbouring resonators.

(Some figures may appear in colour only in the online journal)

1. Introduction

During the last two decades, much effort has been devoted to the study of phononic crystals—two- or three-dimensional periodic arrangements of inclusions in a matrix [1–3]—spurring further interest in the field of acoustic and elastic wave propagation in periodic materials and structures. The fundamental interest of controlling the flow of elastic energy by phononic crystals and its subsequent foreseeable applications are now well established. Studies of propagation in two- or three-dimensional phononic crystals include the analysis of frequency band gaps as well as the confinement and guiding of elastic energy through the use of defect inclusions in perfect phononic crystal structures [4–8]. Most phononic crystal waveguides are formed from line defects [9–11]. Line defects indeed open transmission channels within the otherwise completely opaque complete band gaps of perfect crystals. The dispersion of guided waves inside the frequency band gap is usually multimodal. Dramatic interference effects can then appear between different guided bands, leading to phenomena such as mini-band gaps, avoided crossings, and band repelling [12–14]. Another guiding mechanism, which is less examined, is the coupling of defect cavities in phononic crystals [15–17]. These structures, which we refer to as coupled-resonator acoustic waveguides (CRAWs), provide one with increased flexibility in the design of their dispersion relation, by using only the geometrical parameters defining the cavities and their coupling mechanism [16, 18].

The idea of CRAWs, followed by analogy with coupled-cavity waveguides (CCWs) or coupled-resonator optical waveguides (CROWs), formed in photonic crystals [19–24]. Among the various mechanisms that have been proposed for the guiding of optical waves in photonic crystals, wave propagation in a chain of evanescently coupled optical resonators is both simple and efficient. Independent of the type of resonator and technology, the concept underlying

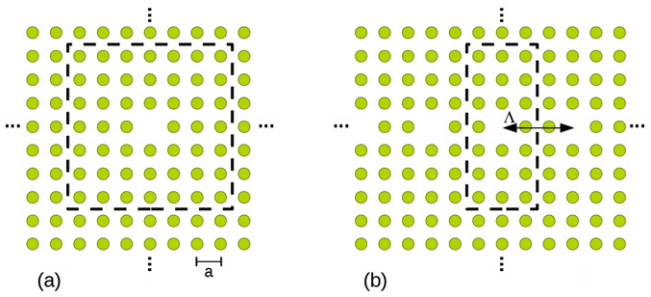

Figure 1. (*a*) Schematic of a cavity formed by a single point defect of a square-lattice phononic crystal. The lattice constant is a. (*b*) Schematic of a coupled-resonator acoustic waveguide (CRAW) created in the same phononic crystal, where Δ is the separation between point defect cavities. The dashed lines indicate the boundaries of the super-cells used for band structure computations.

slow light propagation in a CROW is the forced recirculation of light between resonators [20]. The dispersion relation, and hence the group velocity, can be tuned by varying the coupling strength between cavities, for instance by changing their separation. Propagation in CROWs has been described either by using the tight-binding approximation (for cavities) [19, 20, 25, 26] or by means of the transfer-matrix method (for rings) [23, 27]. In this paper, we discuss the CRAW relation dispersion in the context of coupled cavities created by introducing point defects in phononic crystals, based on both the tight-binding model [20] and *via* an alternative approach inspired by models of phonon propagation in linear chains of atoms. The discussion is illustrated with the case of CRAWs in a two-dimensional solid–solid square-lattice phononic crystal composed of tungsten inclusions in a silicon matrix. It is especially found that the CRAW dispersion relation can be described with only a few harmonics in a Fourier series expansion whose Fourier coefficients are a direct measure of the coupling of neighbouring resonators.

2. Numerical CRAW dispersion

Let us first illustrate in this section the CRAW concept using the example of a two-dimensional (2D) square-lattice array of tungsten inclusions embedded in a silicon matrix. Although the structure is 2D, the results could be extrapolated to 3D without difficulty. A complete phononic band gap is known to exist in this crystal [28] for a range of filling fractions. Material constants for tungsten and silicon are taken from [28]. With the filling fraction $f = \pi r^2/a^2 = 0.145$, the complete band gap extends in the range $\omega a/(2\pi) = 2234$–$2664\,\mathrm{m\,s^{-1}}$, with a the lattice constant, r the inclusion radius, and ω the angular frequency. Cavities can be created by locally removing one inclusion, thus creating a point defect in the crystal as depicted in figure 1(*a*). When the number of inclusions separating two cavities is large enough, they can be thought of as isolated or uncoupled. When the separation between cavities Λ is is not too large, as depicted in figure 1(*b*), the evanescent fields extending outside the cavities can couple them, thus creating a channel for guided waves.

The band structure of the perfect phononic crystal is shown in figure 2(*a*). For the particular tungsten–silicon

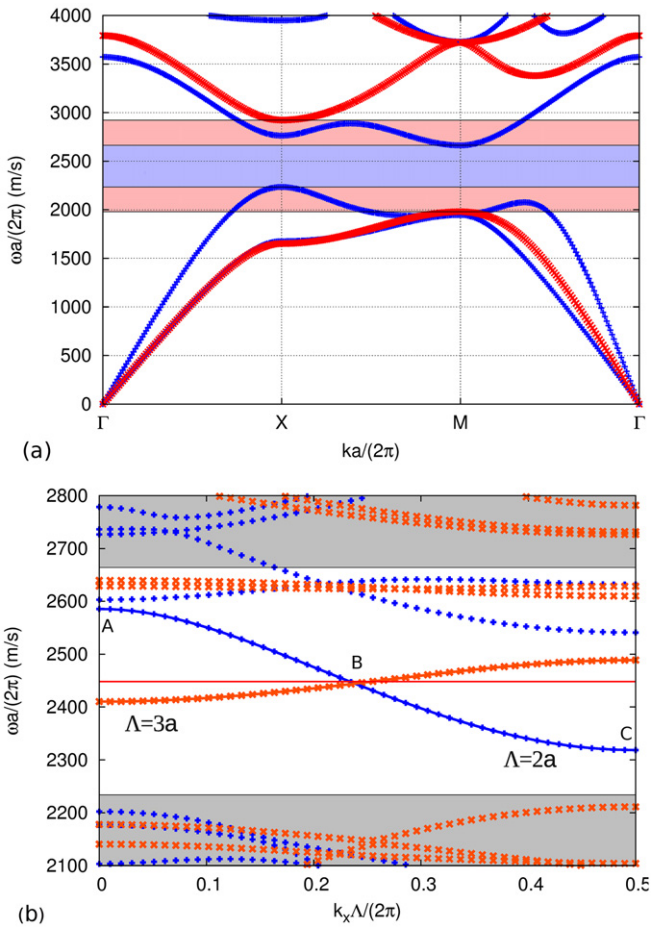

Figure 2. (*a*) Band structure of a phononic crystal composed of a 2D square-lattice array of cylindrical tungsten inclusions embedded in a silicon matrix, with a filling fraction of 0.145. The reduced frequency $\omega a/(2\pi)$ is plotted as a function of the reduced wavenumber $ka/(2\pi)$ varying along the contour of the irreducible Brillouin zone. Shear waves linearly polarized along the inclusion axis (red crosses) are completely decoupled from in-plane polarized waves (blue crosses). The complete band gap (blue area) is contained within the pure-shear band gap (red area). (*b*) CRAW dispersion for cavity separation $\Lambda = 2a$ (blue crosses) and for $\Lambda = 3a$ (orange crosses). The red horizontal line at $\Omega a/(2\pi) = 2448\,\mathrm{m\,s^{-1}}$ indicates the resonant frequency of the isolated phononic crystal cavity. The phononic band gap range is limited by the grey regions.

composition considered here, shear waves that are linearly polarized along the inclusion axis are completely decoupled from the in-plane polarized waves. The pure-shear band gap is larger than the complete band gap and contains it. The dispersion relation of the CRAW can be adequately calculated using a super-cell approach with periodic boundary conditions. The practical implementation was performed with the finite element method (FEM), following the scheme presented by Hussein for incorporating the wavevector dependence [29]. For the phononic crystal cavity in figure 1(*a*), we considered a square super-cell of size $7a \times 7a$, i.e. adjacent cavities are separated by six inclusions, which was found to be sufficient for removing any noticeable coupling between cavities. The resonant frequency of the phononic crystal cavity is $\Omega a/(2\pi) = 2448\,\mathrm{m\,s^{-1}}$, close to the center of

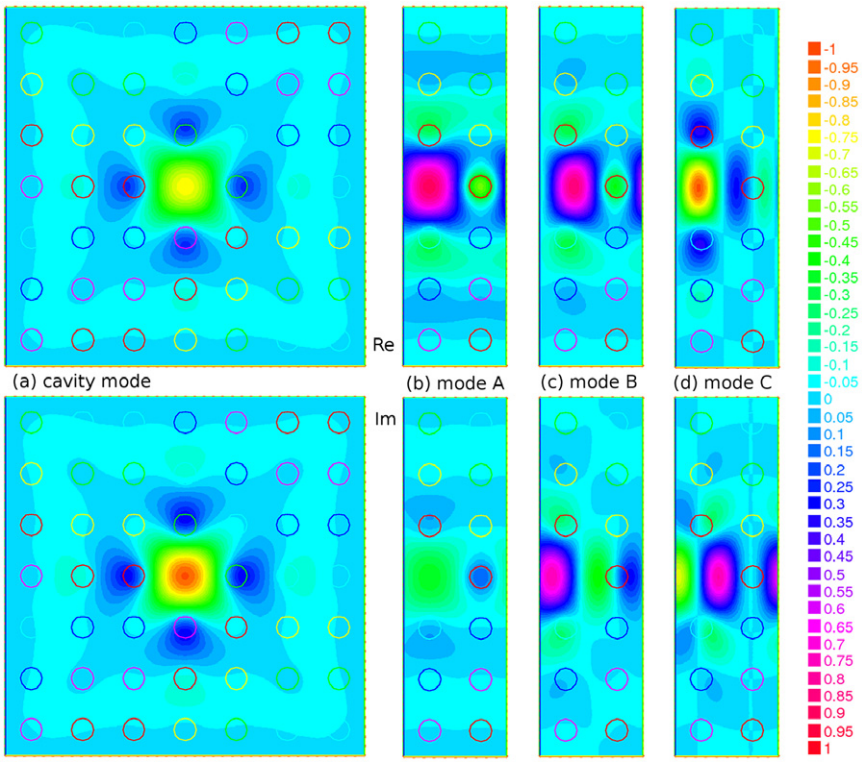

Figure 3. (*a*) Displacement field distribution for the mode of an isolated cavity created by a single defect in a phononic crystal. The phononic crystal is a 2D square-lattice array of cylindrical tungsten inclusions embedded in a silicon matrix with a filling fraction of 0.145. (*b*) Displacement field distributions for mode A ($k_x\Lambda = 0$), (*c*) mode B ($k_x\Lambda = \pi/2$) and (*d*) mode C ($k_x\Lambda = \pi$), for a CRAW with cavity separation $\Lambda = 2a$. Letters A, B and C refer to the labelling in figure 2. The polarization of all modes is pure shear. The real part is displayed on the first line and the imaginary part on the second. Modes are arbitrarily but consistently normalized.

the complete band gap, and the resonant wave is pure-shear polarized. For the CRAW, the super-cell has a size $\Lambda \times 7a$. Figure 2(*b*) shows the computed band structure in the X direction when $\Lambda = 2a$ and $\Lambda = 3a$, i.e. when the coupled cavities are separated by 1 or 2 inclusions, respectively. In both cases, guided propagation is not monomodal and a total of three guided modes are found inside the complete band gap. CRAW behaviour is clearly observed around the isolated cavity resonant frequency $\Omega a/(2\pi) = 2448\,\mathrm{m\,s^{-1}}$: the dispersion relation oscillates gently. It was further verified that the polarization is pure shear, as for the isolated cavity mode shown in figure 3(*a*). The amplitude of frequency variations is clearly dependent on the coupling strength, as expected. There are also two degenerate phononic crystal cavity modes at resonant frequency $\Omega a/(2\pi) = 2625\,\mathrm{m\,s^{-1}}$. They give rise to CRAW behaviour as well, but with dispersion relations that are strongly influenced by the proximity of the phononic bands just above the band gap. They will not be considered further in this paper.

The CRAW dispersion reaches extrema for both $k_x\Lambda = 0$ and $k_x\Lambda = \pi$, and crosses the isolated cavity line close to $k_x\Lambda = \pi/2$. Figure 3 displays modal shapes for these particular values of the wavenumber, for $\Lambda = 2a$. At point A, $k_x\Lambda = 0$, neighbouring cavities oscillate in phase. The field distribution in this case, shown in figure 3(*b*), is centered on the defects and resembles the isolated cavity field distribution, shown in figure 3(*a*), but is spatially compressed in the propagation direction by cavity coupling; hence the stored energy in the cavity increases and so does the frequency. In the case $\Lambda = 3a$, shown in figure 4(*a*), the converse happens: the field distribution expands outside the defect, causing the stored energy and the frequency to decrease. At point C, $k_x\Lambda = \pi$, the boundary condition between adjacent cavities is anti-periodic ($\exp(-\mathrm{i}k_x\Lambda) = -1$). The field distributions shown in figure 3(*d*) and in figure 4(*c*), in this case, indicate that neighbouring cavities oscillate in phase opposition, though not simply according to the isolated cavity field distribution, as evidenced by the imaginary part of the displacement field. Point B, $k_x\Lambda = \pi/2$, is exactly mid-way between symmetry points A and C. If the dispersion relation were perfectly symmetric, we would expect the CRAW frequency at point B to equal the isolated cavity resonant frequency. This is almost verified for $\Lambda = 3a$, but not for $\Lambda = 2a$. This deviation from symmetry is discussed in the following section. Finally, considering the field distributions in figure 3(*c*) and in figure 4(*b*), we remark that the real part and the imaginary part of the displacement are in quadrature: $\exp(-\mathrm{i}k_x\Lambda) = -\mathrm{i}$ and hence real and imaginary parts are continuously exchanged at the boundaries of the super-cell.

3. CRAW dispersion relation

3.1. Tight-binding model

Yariv *et al* proposed a direct derivation of the dispersion relation of a CROW [20] based on the tight-binding model of quantum mechanics [30, 31]. In this sub-section, we

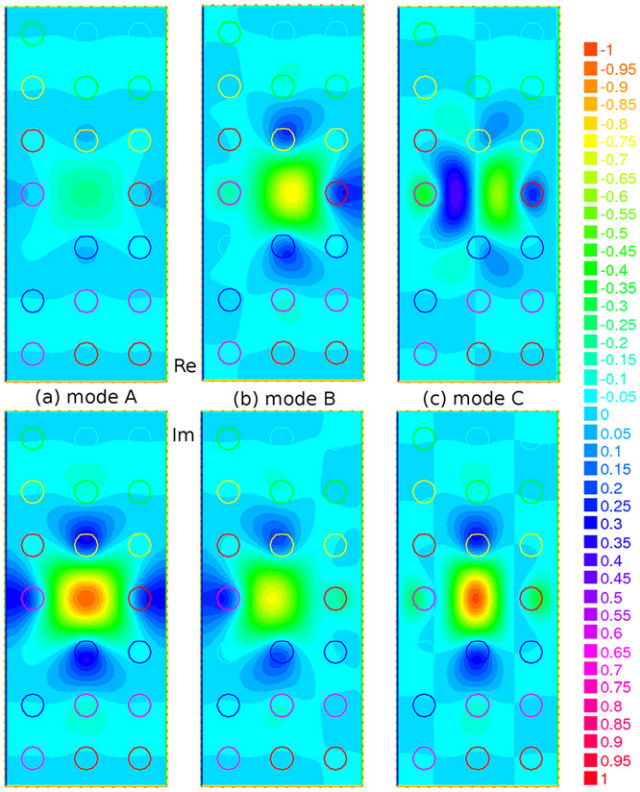

Figure 4. (*a*) Displacement field distributions for mode A ($k_x\Lambda = 0$), (*b*) mode B ($k_x\Lambda = \pi/2$) and (*c*) mode C ($k_x\Lambda = \pi$), for the CRAW with cavity separation $\Lambda = 3a$. Letters A, B and C refer to the labelling in figure 2. The polarization of all modes is pure shear. The real part is displayed on the first line and the imaginary part on the second. Modes are arbitrarily but consistently normalized.

extend the method to the phononic crystal CRAW case. The tight-binding model is used in solid state physics to explain the electronic band structure of insulators. It applies when the overlap of atomic wave functions is enough to require a correction to the picture of isolated atoms, but not so much as to render the atomic description completely irrelevant. It follows, therefore, that when an electron is captured by an ion during its motion through the lattice, the electron remains there for a long time before leaking, or tunneling, to the next ion. The probability of tunneling is measured with the overlapping between the electron wave functions of isolated atoms. The basic idea for a CROW or a CRAW is then to look for the guided mode as a weighted superposition of resonant modes attached to a cavity site, with the weights depending on the wavenumber. Replacing this *ansatz* in the wave equation of the periodic structure, a dispersion relation linking the frequency and the wavenumber of the guided wave can be obtained explicitly. The coefficients appearing in the dispersion relation can be found from overlap integrals involving the cavity mode distribution, much as in the original tight-binding model.

We consider two different spatial domains explicitly, one on which the CRAW is defined (i.e. the real spatial structure of the CRAW shown in figure 1(*b*)) and one on which the cavity mode is defined (i.e. the super-cell containing a defect of an otherwise perfectly periodic crystal shown in figure 1(*a*)). On the one hand, the isolated cavity mode u_0 at resonant angular frequency Ω satisfies the elastodynamic equation

$$-\nabla\cdot(c_0\nabla u_0) = \Omega^2\rho_0 u_0, \tag{1}$$

where c_0 and ρ_0 are defined on the cavity super-cell. c_0 is the rigidity tensor and ρ_0 is the mass density; both quantities are spatially discontinuous at each interface between an inclusion and the matrix. ∇u_0 is the gradient of the displacement field and $\nabla\cdot()$ denotes the divergence operator. Left-multiplying by the conjugate transpose of u_0 and integrating over the domain, we have in bra-ket notation (scalar product)

$$-\langle u_0|\nabla\cdot(c_0\nabla u_0)\rangle = \Omega^2\langle u_0|\rho_0 u_0\rangle. \tag{2}$$

Further integrating this relation by parts, this is just the statement that potential energy equals kinetic energy for a mode

$$\langle\nabla u_0|c_0\nabla u_0\rangle = \Omega^2\langle u_0|\rho_0 u_0\rangle. \tag{3}$$

On the other hand, the CRAW mode also satisfies the elastodynamic equation but on the CRAW domain instead of the single cavity domain,

$$-\nabla\cdot(c\nabla u) = \omega^2\rho u, \tag{4}$$

c and ρ are defined on the CRAW domain and are again spatially discontinuous. The tight-binding *ansatz* is the assumption that

$$u = \sum_n \exp(-\mathrm{i}kx_n)T_n u_0, \tag{5}$$

where $x_n = n\Lambda$ is the coordinate of the nth resonator and T_n is the translation operator from the origin to location x_n. This expression means that the guided mode is approximated by a superposition of translated cavity modes, each having the same weight in modulus but a relative phase kx_n. As we indicated before, u_0 and u are not defined on the same spatial domains and there is inevitably an implied approximation where both domains differ. It should be noted that the superposition as written is so far unnormalized. We impose the normalization $\langle u_0|\rho_0 u_0\rangle = 1$, which in turn implies $\langle\nabla u_0|c_0\nabla u_0\rangle = \Omega^2$ from (3). Projecting (4) on the resonant mode, we have

$$\langle\nabla u_0|c\nabla u\rangle = \omega^2\langle u_0|\rho u\rangle. \tag{6}$$

Substituting (5) in (6) results in a dispersion relation of the form $\omega(k)$,

$$\omega^2 = \frac{\beta_0 + \Delta\beta + \sum_{n\neq 0}\exp(-\mathrm{i}kn\Lambda)\beta_n}{1 + \Delta\alpha + \sum_{n\neq 0}\exp(-\mathrm{i}kn\Lambda)\alpha_n}, \tag{7}$$

with the coefficients

$$\beta_0 = \langle\nabla u_0|c_0\nabla u_0\rangle = \Omega^2, \tag{8}$$

$$\Delta\beta = \langle\nabla u_0|\Delta c\nabla u_0\rangle, \tag{9}$$

$$\beta_n = \langle\nabla u_0|c\nabla T_n u_0\rangle, \tag{10}$$

$$\Delta\alpha = \langle u_0|\Delta\rho u_0\rangle, \tag{11}$$

$$\alpha_n = \langle u_0|\rho T_n u_0\rangle. \tag{12}$$

Table 1. Coefficients of the tight-binding dispersion relation as computed from the cavity mode of figure 3.

CRAW	$a^2\beta_0/(2\pi)^2$ ($m^2\,s^{-2}$)	$\Delta\alpha$ (w.u.)	$a^2\Delta\beta/(2\pi)^2$ ($m^2\,s^{-2}$)	α_1 (w.u.)	$a^2\beta_1/(2\pi)^2$ ($m^2\,s^{-2}$)
$\Lambda = 2a$	5993756	−0.00806	−15140	0.0454	566299
$\Lambda = 3a$	5993756	−0.000513	−1937	0.00315	−44451

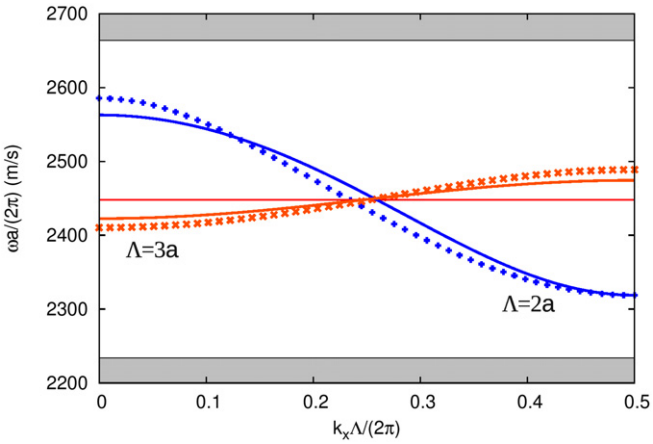

Figure 5. Comparison of the computed CRAW dispersion relation (plus and cross signs) with the tight-binding dispersion relation, with coefficients given in table 1 (solid lines). The phononic crystal is a 2D square-lattice array of cylindrical tungsten inclusions embedded in a silicon matrix with a filling fraction of 0.145. Blue plus signs and solid line: $\Lambda = 2a$. Orange cross signs and solid line: $\Lambda = 3a$.

By definition, $\Delta c = c - c_0$ and $\Delta\rho = \rho - \rho_0$ are non-vanishing only where the CRAW domain and the cavity domain differ. The coefficients α_n and β_n are obtained from overlap integrals involving the cavity mode and its translated copies; they can be loosely viewed as coupling coefficients between neighbouring cavities.

The coupling coefficients in equations (8)–(12) were estimated from the cavity mode shown in figure 3(*a*) and are reported in table 1 for $\Lambda = 2a$ and $\Lambda = 3a$. These values are used in figure 5 to compare the estimated dispersion relation with the one computed in section 2. It can be seen that the agreement is only partial: although the general trends are reproduced, the precise frequency dispersion is not recovered. As a possible explanation, we point out the differences in the definitions of the CRAW and the cavity domains. The cavity mode and its translated versions are defined for the cavity domain but used on the CRAW domain in (9)–(12). As the material constants of tungsten and silicon are quite different in magnitude, notable differences must indeed result. Such differences could already be observed in figure 3, from which it appears that the field distributions for the guided mode at points A, B and C clearly differ from the simple superposition postulated in (5).

3.2. Linear chain of coupled resonators

From the results in the previous sub-section, it is clear that the tight-binding model contains an assumption that is too strong in the case of the CRAW defined in a phononic crystal: the guided wave cannot be trustfully represented as a linear superposition of resonant modes. We consider here an alternative model where we describe the coupled cavities as a linear chain of coupled harmonic oscillators, similar to the description of phonon propagation in a one-dimensional lattice of atoms. A quantum treatment of the problem would require constructing the Hamiltonian of the CRAW as a sum of the Hamiltonians of isolated resonators plus an interaction Hamiltonian describing the interaction of coupled resonators [31]. Here, we alternatively postulate the following simple classical model

$$-\frac{\mathrm{d}^2 U_n}{\mathrm{d}t^2} = \sum_{m=-\infty}^{\infty} \gamma_m U_{n+m}. \tag{13}$$

In this equation, U_n is a scalar variable similar to a displacement from equilibrium position describing the state of the resonator. γ_0 equals the square of the resonant angular frequency Ω^2 in the decoupling limit, and the γ_m for $m \neq 0$ are coupling constants with the same units as γ_0. The underlying assumption is that the response to small perturbations of the equilibrium positions of resonators is linear and translation invariant, hence the convolution operation on the right-hand side. Note that these assumptions are much weaker than the tight-binding assumption (5) that the guided mode is a superposition of translated cavity modes. Next we consider the discrete Fourier transform (DFT) of the sequence U_n

$$\bar{U}(k) = \sum_n U_n \exp(\mathrm{i}kn\Lambda) \tag{14}$$

and its inverse

$$U_n = \frac{\Lambda}{2\pi}\int_{-\pi/\Lambda}^{\pi/\Lambda} \mathrm{d}k\,\bar{U}(k)\exp(-\mathrm{i}kn\Lambda). \tag{15}$$

In these relations, the wavenumber k is a real variable defined in the first Brillouin zone. Making use of the orthonormality and completeness of the DFT, the following dispersion relation is obtained upon substituting (15) in (13)

$$\omega^2 = \sum_{m=-\infty}^{\infty} \gamma_m \exp(-\mathrm{i}km\Lambda). \tag{16}$$

For a symmetric CRAW, the dispersion relation simplifies to

$$\omega^2 = \gamma_0 + \sum_{m=1}^{\infty} 2\gamma_m \cos(km\Lambda). \tag{17}$$

We have thus obtained the dispersion relation as a Fourier series, similarly to the tight-binding result (7). In contrast, however, the coupling coefficients γ_m are not known beforehand, but they can be fitted from the computed

Table 2. Coefficients of the linear chain of coupled resonators dispersion relation, as obtained by fitting the computed CRAW dispersion relation of figure 2.

CRAW	$\Gamma_0 a/(2\pi)$ (m s^{-1})	$\Gamma_1 a/(2\pi)$ (m s^{-1})	$\Gamma_2 a/(2\pi)$ (m s^{-1})	$\Gamma_3 a/(2\pi)$ (m s^{-1})
$\Lambda = 2a$	2443.16	131.30	8.47	2.08
$\Lambda = 3a$	2448.34	−39.15	1.17	−0.13

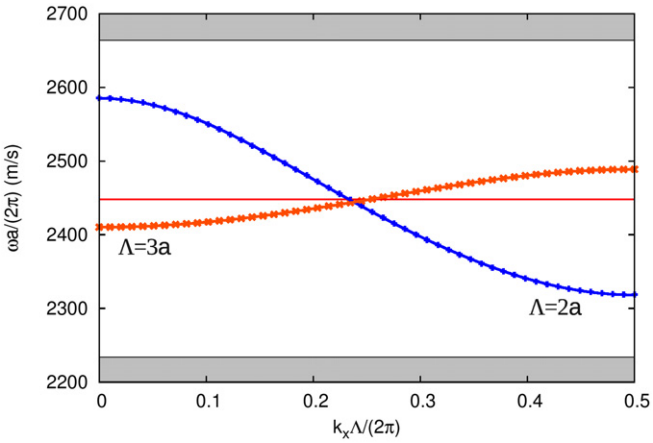

Figure 6. Comparison of the computed CRAW dispersion relation (plus and cross signs) with the linear chain of coupled resonators dispersion relation, with coefficients given in table 2 (solid lines). The phononic crystal is a 2D square lattice array of cylindrical tungsten inclusions embedded in a silicon matrix with a filling fraction of 0.145. Blue plus signs and solid line: $\Lambda = 2a$. Orange cross signs and solid line: $\Lambda = 3a$.

dispersion relation. We further remark that we can express directly the angular frequency as a Fourier series

$$\omega = \Gamma_0 + \sum_{m=1}^{\infty} 2\Gamma_m \cos(km\Lambda), \tag{18}$$

where the coefficients Γ_m are straightforwardly obtained from the coefficients γ_m. A similar formula, but with the summation limited to $m = 1$ and $\Gamma_0 = \Omega_0$, was proposed by Sainidou *et al* for fluid–fluid phononic crystals [16]. Our example computation is for pure-shear waves in a solid–solid phononic crystal, which can be shown to obey an inhomogeneous scalar wave equation, as do pressure waves in fluid–fluid phononic crystals. It is then not surprising that different systems can be described with similar dispersion relations. We are furthermore confident that the case of generally polarized elastic waves can be described similarly. As a further remark, our linear chain of coupled resonators dispersion relation (18) does not impose $\Gamma_0 = \Omega_0$ and does not limit the Fourier series to only one harmonic. The former property is necessary to account for CRAW dispersion relations that are not symmetric with respect to the isolated cavity frequency, as we exemplified in section 2. The latter property introduces anharmonicity in the model, which is necessary to account for cavity coupling beyond nearest neighbours.

Table 2 gives the numerical values that were obtained by fitting the computed CRAW dispersion relations to (18). It can be observed that the Fourier series converges very quickly, in accordance with the intuition that only neighbouring cavities have influence on the dispersion of waves guided by resonator coupling. Figure 6 compares the computed dispersion relation with the theoretical dispersion relation (18). An excellent agreement is obtained with only the first 4 Fourier coefficients included, or with couplings included up to the third neighbouring resonator. It can be remarked that the property that dispersion relations can be represented by Fourier series expansions is implied by periodicity and linearity alone, and independently of the CRAW concept. As a consequence, relations (17) or (18) could have been postulated from the start. The significance of the model (13), however, is that the Fourier coefficient γ_m can be directly identified as a measure of the coupling of a cavity with its m-th neighbour. The fast decrease of the coupling coefficients then directly dictates the smoothness of the CRAW dispersion relation and the amplitude of its frequency variations.

4. Conclusion

We have presented an analysis of the dispersion relation of CRAWs in phononic crystals. While the dispersion relation could be computed accurately based on a super-cell technique, we examined two different analytical models based on the tight-binding approximation, on the one hand, and on a 1D-lattice of linearly coupled resonators, on the other hand. Both models predict that angular frequency ω as a function of the wavenumber k has the form of a Fourier series in $\exp(-ik\Lambda)$, with Λ the separation between resonators. Of the two models, only the tight-binding approximation gives an explicit expression for the Fourier coefficients. It was found, however, not to faithfully reproduce the exact dispersion relation, which we attributed to the consequent domain modification that occurs when forming the CRAW from the isolated cavity. This modification is indeed incompatible with the tight-binding assumption that the guided mode can be represented as a linear superposition of isolated cavity modes. The linear chain of coupled resonators model, in contrast, has *a priori* unspecified coefficients that can be fitted against the computed dispersion relation. It was found that only a very limited number of Fourier coefficients are necessary to reproduce the exact dispersion and that the mth Fourier coefficient can be identified as a direct measure of the coupling of a cavity with its mth neighbour. The fast decrease in Fourier coefficients is then simply a consequence of the fast decrease of the influence of distant resonators. CRAWs are promising in order to get slow-wave phononic waveguides whose dispersion can be tuned by changing the coupling strength between resonators. The design of simultaneous CRAW-CROW structures could have strong potential for optomechanics and enhanced light and sound interactions in phoxonic crystals [32].

Acknowledgments

Financial support from the European Community's Seventh Framework program (FP7/2007-2013) under grant agreement number 233883 (TAILPHOX) is gratefully acknowledged. VL

acknowledges the support of the Labex ACTION program (contract ANR-11-LABX-01-01).

References

[1] Sigalas M M and Economou E N 1993 Band structure of elastic waves in two dimensional systems *Solid State Commun.* **86** 141–3

[2] Kushwaha M S, Halevi P, Dobrzynski L and Djafari-Rouhani B 1993 Acoustic band structure of periodic elastic composites *Phys. Rev. Lett.* **71** 2022–5

[3] Miyashita T 2005 Sonic crystals and sonic wave-guides *Meas. Sci. Technol.* **16** R47–63

[4] Khelif A, Djafari-Rouhani B, Vasseur J-O and Deymier P A 2003 Transmission and dispersion relations of perfect and defect-containing waveguide structures in phononic band gap material *Phys. Rev.* B **68** 024302

[5] Sun J-H and Wu T-T 2007 Propagation of acoustic waves in phononic-crystal plates and waveguides using a finite-difference time-domain method *Phys. Rev.* B **76** 104304

[6] Vasseur J O, Hladky-Hennion A-C, Djafari-Rouhani B, Duval F, Dubus B, Pennec Y and Deymier P A 2007 Waveguiding in two-dimensional piezoelectric phononic crystal plates *J. Appl. Phys.* **101** 114904

[7] Hsiao F-L, Khelif A, Moubchir H, Choujaa A, Chen C-C and Laude V 2007 Waveguiding inside the complete band gap of a phononic crystal slab *Phys. Rev.* E **76** 056601

[8] Wu T-C, Wu T-T and Hsu J-C 2009 Waveguiding and frequency selection of lamb waves in a plate with a periodic stubbed surface *Phys. Rev.* B **79** 104306

[9] Khelif A, Choujaa A, Benchabane S, Djafari-Rouhani B and Laude V 2004 Guiding and bending of acoustic waves in highly confined phononic crystal waveguides *Appl. Phys. Lett.* **84** 4400–2

[10] Li X-C and Liu Z-G 2005 Bending and branching of acoustic waves in two-dimensional phononic crystals with linear defects *Phys. Lett.* A **338** 413–9

[11] Romero-García V, Vasseur J O, Hladky-Hennion A C, Garcia-Raffi L M and Sánchez-Pérez J V 2011 Level repulsion and evanescent waves in sonic crystals *Phys. Rev.* B **84** 212302

[12] Wu T-T and Huang Z-G 2004 Level repulsions of bulk acoustic waves in composite materials *Phys. Rev.* B **70** 214304

[13] Achaoui Y, Khelif A, Benchabane S and Laude V 2010 Polarization state and level repulsion in two-dimensional phononic crystals and waveguides in the presence of material anisotropy *J. Phys. D: Appl. Phys.* **43** 185401

[14] Romero-García V, Sánchez-Pérez J V and Garcia-Raffi L M 2010 Propagating and evanescent properties of double-point defects in sonic crystals *New J. Phys.* **12** 083024

[15] Khelif A, Choujaa A, Djafari-Rouhani B, Wilm M, Ballandras S and Laude V 2003 Trapping and guiding of acoustic waves by defect modes in a full-band-gap ultrasonic crystal *Phys. Rev.* B **68** 214301

[16] Sainidou R, Stefanou N and Modinos A 2006 Linear chain of weakly coupled defects in a three-dimensional phononic crystal: a model acoustic waveguide *Phys. Rev.* B **74** 172302

[17] Khelif A, Mohammadi S, Eftekhar A A, Adibi A and Aoubiza B 2010 Acoustic confinement and waveguiding with a line-defect structure in phononic crystal slabs *J. Appl. Phys.* **108** 084515

[18] Benchabane S, Khelif A, Choujaa A, Djafari-Rouhani B and Laude V 2005 Interaction of waveguide and localized modes in a phononic crystal *Europhys. Lett.* **71** 570–5

[19] Stefanou N and Modinos A 1998 Impurity bands in photonic insulators *Phys. Rev.* B **57** 12127–33

[20] Yariv A, Xu Y, Lee R K and Scherer A 1999 Coupled-resonator optical waveguide: a proposal and analysis *Opt. Lett.* **24** 711

[21] Xu Y, Lee R K and Yariv A 2000 Propagation and second-harmonic generation of electromagnetic waves in a coupled-resonator optical waveguide *J. Opt. Soc. Am.* B **17** 387

[22] Olivier S, Smith C, Rattier M, Benisty H, Weisbuch C, Krauss T, Houdré R and Oesterlé U 2001 Miniband transmission in a photonic crystal coupled-resonator optical waveguide *Opt. Lett.* **26** 1019

[23] Melloni A, Morichetti F and Martinelli M 2003 Linear and nonlinear pulse propagation in coupled resonator slow-wave optical structures *Opt. Quantum Electron.* **35** 365–79

[24] Martínez A, García J, Sanchis P, Cuesta-Soto F, Blasco J and Martí J 2007 Intrinsic losses of coupled-cavity waveguides in planar-photonic crystals *Opt. Lett.* **32** 635–7

[25] Grgić J, Campaioli E, Raza S, Bassi P and Mortensen N A 2011 Coupled-resonator optical waveguides: Q-factor and disorder influence *Opt. Quantum Electron.* **42** 511–9

[26] Datta S 1995 *Electronic Transport in Mesoscopic Systems* (Cambridge: Cambridge University Press)

[27] Poon J, Scheuer J, Mookherjea S, Paloczi G T, Huang Y-Y and Yariv A 2004 Matrix analysis of microring coupled-resonator optical waveguides *Opt. Express* **12** 90

[28] Khelif A, Wilm M, Laude V, Ballandras S and Djafari-Rouhani B 2004 Guided elastic waves along a rod-defect of a two-dimensional phononic crystal *Phys. Rev.* E **69** 067601

[29] Hussein M I 2009 Reduced Bloch mode expansion for periodic media band structure calculations *Proc. R. Soc.* A **465** 2825–48

[30] Omar M A 1993 *Elementary Solid State Physics: Principles and Applications* (New York: Addison-Wesley)

[31] Hu F M, Lan Zhou, Tao Shi and Sun C P 2007 Coupled cavity qed for coherent control of photon transmission: Green-function approach for hybrid systems with two-level doping *Phys. Rev.* A **76** 013819

[32] Laude V, Beugnot J-C, Benchabane S, Pennec Y, Djafari-Rouhani B, Papanikolaou N, Escalante J M and Martinez A 2011 Simultaneous guidance of slow photons and slow acoustic phonons in silicon phoxonic crystal slabs *Opt. Express* **19** 9690–8